

The mass transfer parameter and recovery factor are calculated by interpolation between the laminar and turbulent values in terms of the factor

$$F = \log_{10}(St_r/St_L)/\log_{10}(K_r St_r/St_L) \quad (6)$$

The transitional heating regime corresponds to  $0 < F < 0.99$ .

### Growth of Monitored Surface Roughness

Between the initial and the maximum roughness dimensions [assumption (5)], the surface-roughness growth rate may be expressed as a function of pressure, Reynolds number, surface roughness, surface recession rate, and other variables:

$$dk/dt = f(p, Re, k, dN/dt, \dots) \quad (7)$$

Before the functional form is determined by extensive theoretical and experimental studies, the following relationship may be considered ( $n > 1$ ):

$$\frac{dk}{dt} = \begin{cases} [(k - k_{\min})/(k_c - k_{\min})]^{1/n} (dN/dt), & k_{\min} < k \leq k_c \\ [(k_{\max} - k)/(k_{\max} - k_c)]^{1/n} (dN/dt), & k_c < k < k_{\max} \end{cases} \quad (8)$$

Integration of Eq. (8) between limits  $k_{\min}$  and  $k_{\max}$  yields

$$\Delta N = [n/(n-1)](k_{\max} - k_{\min}) \quad (9)$$

The case  $n \rightarrow \infty$  corresponds to the upperlimit roughness growth rate, provided no surface fracture occurs. On the other hand, zero growth rate corresponds to  $n = 1$ .

### Application of Methods

The present method is used to predict the heat-transfer rate on roughened hemispheres and cones presented recently by Thyson et al.<sup>12</sup> Reasonable agreements between prediction and data are obtained, as shown in Figs. 1 and 2.

Experimental data have not been found to validate the assumption on surface roughness growth. Nevertheless, Eqs. (8) and (9) may be used in parametric sensitivity studies, particularly when an approximate estimate of the magnitude of recessions is available.

### References

- <sup>1</sup> Schlichting, H., *Boundary Layer Theory*, 4th ed., McGraw-Hill, New York, 1960, pp. 457-565.
- <sup>2</sup> Welsh, W. E., Jr., "Shape and Surface Roughness Effects on Turbulent Nose Tip Ablation," AIAA Paper 69-717, San Francisco, Calif., 1969.
- <sup>3</sup> Fenton, F. W., "The Turbulent Boundary Layer on Uniformly Rough Surfaces at Supersonic Speeds," Rept. DRL-437, Jan. 1960, Defense Research Lab., The Univ. of Texas, Austin, Texas.
- <sup>4</sup> Nestler, D. E., "Compressible Turbulent Boundary Layer Heat Transfer to Rough Surfaces," AIAA Paper 70-742, Los Angeles, Calif., 1970.
- <sup>5</sup> Strass, H. K. and Tyner, T. W., "Some Effects of Roughness on Stagnation-Point Heat Transfer at a Mach Number of 2, a Stagnation Temperature of 3,530°F, and a Reynolds Number of  $2.5 \times 10^6$  per Foot," RM L58C10, May 1958, NACA.
- <sup>6</sup> Diaconis, N. S., Wisniewski, R. J., and Jack, J. R., "Heat Transfer and Boundary-Layer Transition on Two Blunt Bodies at Mach Number 3.12," TN 4099, Oct. 1957, NACA.
- <sup>7</sup> Dunavant, J. and Stone, H. W., "Effect of Roughness on Heat Transfer to Hemisphere Cylinders at Mach Numbers 10.4 and 11.4," TN D-3871, 1967, NASA.
- <sup>8</sup> Persh, J., "A Procedure for Calculating the Boundary Layer Development in the Region of Transition from Laminar to Turbulent Flow," NAVORD Rept. 4438, March 1957, U. S. Naval Ordnance Lab., White Oak, Md.
- <sup>9</sup> Cresci, R. J., MacKenzie, D. A., and Libby, P. A., "An Investigation of Laminar, Transitional, and Turbulent Heat Transfer on Blunt-Nosed Bodies in Hypersonic Flow," *Journal of the Aerospace Sciences*, Vol. 27, No. 6, June 1960, pp. 401-414.

<sup>10</sup> Laganelli, A. L. and Nestler, D. E., "Surface Ablation Pattern: A Phenomenology Study," *AIAA Journal*, Vol. 7, No. 7, July 1969, pp. 1319-1325.

<sup>11</sup> Dipprey, D. F. and Sabersky, R. H., "Heat and Momentum Transfer in Smooth and Rough Tubes at Various Prandtl Numbers," *International Journal of Heat and Mass Transfer*, Vol. 6, No. 5, May 1963, pp. 329-353.

<sup>12</sup> Thyson, N., Neuringer, J., Pallone, A., and Chen, K. K., "Nose Tip Shape Change Predictions During Atmospheric Reentry," AIAA Paper 70-827, Los Angeles, Calif., 1970.

## An Experimental Investigation of Superheated Subliming Solid Thruster Performance

W. L. OWENS JR.\*

Lockheed Missiles & Space Company, Sunnyvale, Calif.

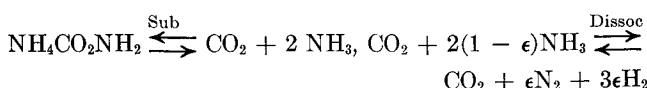
### Introduction

A LIMITATION of subliming solid thrusters has been the relatively low specific impulse obtained at propellant temperatures on the order of 100°F.<sup>1</sup> This Note presents experimental data for a superheated subliming solid thruster which indicate that a considerable improvement in performance is possible through an increase in gas temperature and an attendant reduction in molecular weight. The technology of vapor superheaters has advanced through its application to nitrogen, ammonia, and hydrogen resistojet systems.<sup>2-5</sup> Resistojets are available that will maintain an operating temperature of 1500°F with a heat loss of 12 w (Ref. 4) or 3700°F with a heat loss of ~30 w (Ref. 5). The experimental data presented show that delivered specific impulse ( $I_{sp}$ ) for ammonium carbamate can be suitably predicted using a correlation for nozzle performance that has been shown to correlate most of the available data for throat Reynolds number ( $Re^*$ ) in the range of 100-10,000. Total propulsion system mass as a function of total impulse for two gas temperatures and several thrust levels is shown using predicted  $I_{sp}$ 's.

### Propellant Selection

Most candidate "subliming" solid propellants are ammonium salts which decompose to produce two-four vapor-phase molecules for every solid-phase molecule. Heating the "sublimed" vapor sufficiently causes the  $NH_3$  to dissociate into  $N_2$  and  $H_2$  with an attendant improvement in specific impulse at the expense of the heat of dissociation.

Elimination of the ammonium salts that are toxic, explosive, undergo pyrolysis, or have too low a vapor pressure leaves essentially seven candidate substances: ammonium bicarbonate, -bisulfide, -bisulphite, -carbamate, -carbonate, -sulphide, and -sulphite. Ammonium carbamate was chosen from these because of its low dissociated molecular weight (26 at 100°F, 15.6 at 2000°F), suitable vapor pressure (210 torr at 100°F), and ease of manufacture. The nonelementary sublimation and dissociation reactions for ammonium carbamate ( $NH_4CO_2NH_2$ ) are



Presented as Paper 70-210 at the AIAA 8th Aerospace Sciences Meeting, New York, January 19-21, 1970; submitted October 13, 1970; revision received April 1, 1971.

\* Staff Engineer, Propulsion Systems Department, Space Systems Division.

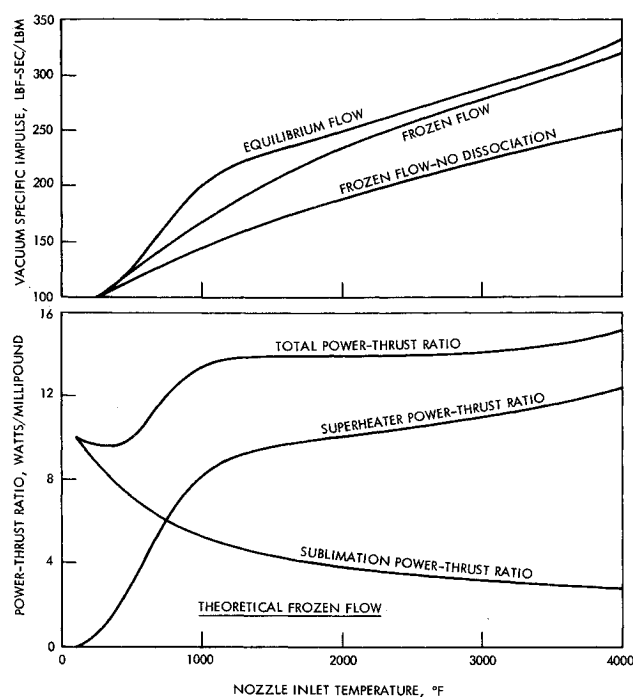


Fig. 1 Vacuum specific impulse and power-thrust ratio for ammonium carbamate with  $P_c = 5$  psia and  $A_c/A^* = 50$ .

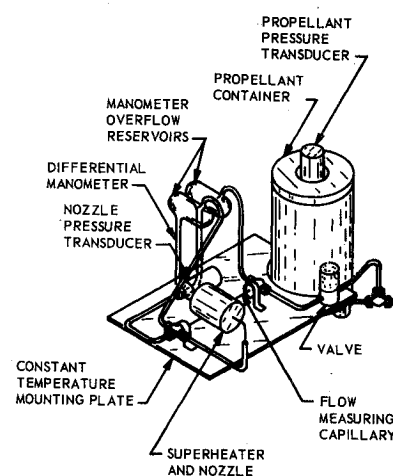
The  $H_2$  produced in the  $NH_3$  dissociation just shown, combines with  $CO_2$  in the "water-gas" reaction to produce the constituents shown in Table 1. Since the water-gas reaction does not involve a change in the total number of moles, the resultant average molecular weight is given by  $\bar{m} = 78/(3 + 2\epsilon)$ . Theoretical  $I_{sp}$  vs temperature for an area ratio of 50 is shown in Fig. 1 (top) for three conditions. These values are ~80 to 85% of those for  $NH_3$  alone. The lower part of Fig. 1 shows the theoretical sublimation and superheater power requirements for superheater equilibrium dissociation and frozen nozzle flow.

The sublimation power-thrust ratio ( $P/F$ ) was calculated by dividing the heat of sublimation by the theoretical  $I_{sp}$  (middle curve Fig. 1 top). The superheater  $P/F$  was obtained by dividing the computed gas enthalpy difference by the theoretical  $I_{sp}$  at various superheated gas temperatures. The actual  $P/F$  will depend on the degree of dissociation and the delivered specific impulse. Estimates of  $P/F$  may be obtained by dividing the values shown in Fig. 1 (bottom) by the ratio of delivered to theoretical  $I_{sp}$ , which is essentially a function of  $Re^*$ .

#### Experimental Apparatus

The thrust system was composed of a propellant container and heater to which a thermal storage resistojet and flow meter were added (Fig. 2). Nozzle pressure was maintained at the desired level during a run with a pressure feedback propellant-heater-controller. Instantaneous mass rates were obtained from a 0.037-in. i.d. capillary flow meter calibrated

Fig. 2 Schematic of experimental apparatus.



with  $N_2$  using an expression from Ref. 1 with an experimentally-determined inlet loss coefficient. The data for  $N_2$  were predictable within  $\pm 3\%$ . A direct thrust measurement device<sup>6</sup> gave an accuracy of approximately  $\pm 4\%$  for thrust. All of the testing was performed in a  $3 \times 3$ -ft vertical vacuum chamber equipped with a 10-in. diffusion pump and a liquid nitrogen cold trap. This provided chamber pressures lower than  $10^{-4}$  torr, which has been found necessary to avoid an anomalous variation in measured thrust.<sup>7</sup> The ammonium carbamate was obtained by combining gaseous  $CO_2$  and  $NH_3$  in a glass resin kettle.

#### Results

Ten runs were made, including three for the purpose of calibrating the capillary flow meter. Capillary and nozzle mass rates were calculated from transient pressure measurements of dry  $N_2$  with isothermal tank blow-down. A plot of nozzle discharge coefficient ( $C_D$ ) vs  $Re^*$  is shown in Fig. 3 (top) for runs 7 and 9. The general conditions for all of the runs are shown in Table 2 (the nozzles had conical divergent sections with  $15^\circ$  half-angles). A correlation of  $C_D$  from Ref. 1 is included in Fig. 3 (top) which shows agreement within the limits of experimental accuracy. Figure 3 (center) shows  $C_D$  vs  $Re^*$  for two runs with ammonium carbamate. The solid and dotted lines indicate the upper and lower limits of calculated  $C_D$  for the cases of no dissociation and thermodynamic equilibrium at the superheater exit, respectively. These  $C_D$  values were calculated from the nozzle mass flow equation using measured values of mass flow rate, nozzle inlet pressure, and temperature, along with the values of chamber molecular weight from Table 1 for the case of thermodynamic equilibrium. Comparison of the experimental data to the  $C_D$  correlation from Ref. 1 indicates that dissociation did not begin until a temperature of approximately  $1200^\circ F$  was attained.

A plot of  $\phi_{sp}$  vs  $Re^*$ , along with the correlation from Ref. 1, is shown in Fig. 3 (bottom);  $\phi_{sp}$  is the ratio of experimental  $I_{sp}$  to the theoretical undissociated frozen flow value. Only data below  $1200^\circ F$  are shown for runs 6 and 10 where the  $NH_3$  is assumed to be undissociated. The variation in  $\phi_{sp}$

Table 1 Theoretical nozzle performance data for ammonium carbamate for  $P_c = 5$  psia and  $A_c/A^* = 50$

Temp., °K	Chamber mol. wt	Vac $I_{sp}$ , sec		Chamber composition, mole %							
		Froz.	Equil.	$CH_4$	$H_2O$	$CO$	$N_2$	$CO_2$	$H_2$	$H$	$OH$
500	22.14	117.1	119.8	20.4	42.2	...	28.2	7.1	1.5	...	...
1000	15.63	193.9	225.6	...	14.0	13.9	20.0	6.1	46.0	...	...
1500	15.62	241.4	257.8	...	17.3	17.3	20.0	2.7	42.7	...	...
2000	15.6	283.0	292.0	...	18.2	18.2	20.0	1.7	41.6	...	...
2500	15.38	321.5	335.6	...	18.0	18.3	19.7	1.4	39.6	2.7	0.3
3000	14.12	363.0	417.3	...	13.8	17.1	18.0	1.0	31.8	15.2	2.2

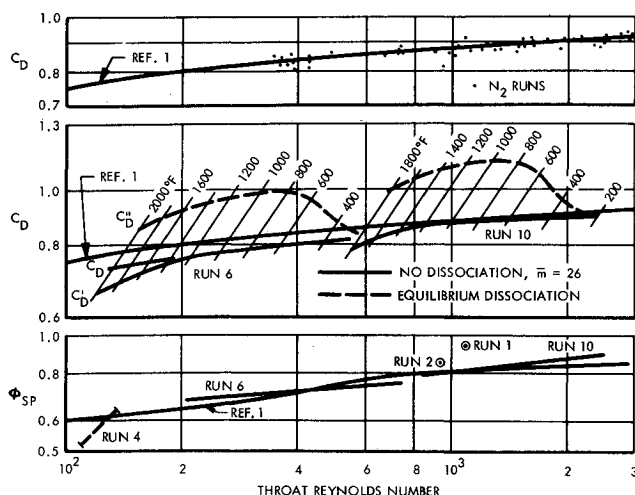


Fig. 3 Experimental discharge coefficients and specific impulse ratio vs throat Reynolds number.

for run 4 results from dividing the experimental  $I_{sp}$  by the theoretical undissociated and dissociated frozen flow values.

### Discussion

The degree of dissociation ( $\epsilon$ ) obtained for runs 6 and 10 was estimated from the following expression

$$\epsilon = \frac{1}{1 - \frac{\bar{m}''}{\bar{m}'}} \left[ 1 - \frac{1}{\left\{ 1 + \frac{C_D - C_D'}{C_D'' - C_D'} \left[ \left( \frac{\bar{m}'}{\bar{m}''} \right)^{1/2} - 1 \right] \right\}^2} \right]$$

where  $\bar{m}$  is the average molecular weight. The single prime refers to the undissociated value of  $\bar{m}$  and  $C_D$  while the double prime represents the value for equilibrium dissociation. The values of  $C_D'$  and  $C_D''$  were obtained from Fig. 3 (middle) for a particular temperature. The unprimed or actual  $C_D$  was obtained by extending the undissociated portion of the data below 1200°F to intersect the various isotherms as shown for Run 6. This relatively simple method of estimating  $\epsilon$  is based on the assumption that the actual value of  $C_D$  for dissociated flow, will follow the general variation with  $Re^*$  given in Ref. 1. It is anticipated that a further increase in temperature above 2000°F would have resulted in the dashed equilibrium dissociation lines decreasing to merge with the projected  $C_D$  curve at the point where complete dissociation was obtained. Values of 35 and 50% were calculated for runs 6 and 10 for an exit temperature of 1800°F. The heater element was a  $2 \times 0.07$ -in. i.d., 18:8 stainless steel tube.

The catalytic dissociation process for the flowing  $NH_3$  within the heated tube can be visualized as being composed of the following four basic mechanisms: 1) counterflow diffusion of  $NH_3$  towards the wall against the dissociation products through the basically stagnant  $CO_2$ ; 2) adsorption of the  $NH_3$  on the surface of the catalyst; 3) the dissociation reaction at active sites on the catalyst; and 4) desorption of  $N_2$  and  $H_2$  from the catalyst surface. Any one or more of the above mechanisms can control the rate of dissociation, resulting in values much less than those calculated for thermo-

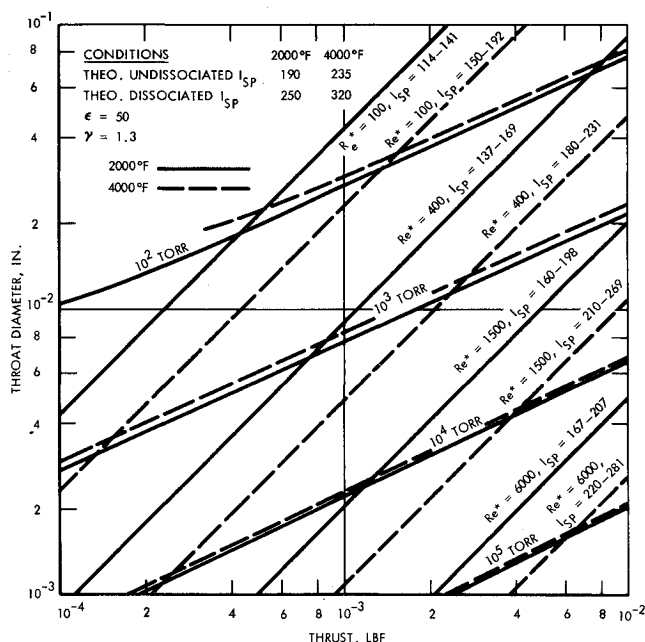


Fig. 4 Delivered specific impulse and nozzle pressure for undissociated and dissociated ammonium carbamate.

dynamic equilibrium. The diffusion rate can be ruled out as the rate-limiting step for the present data since both runs 6 and 9 had approximately the same laminar mass transfer coefficients and gas residence times. It would be possible to explain the greater dissociation for run 10 in terms of the adsorption rate since this is a function of  $NH_3$  concentration, and run 10 had a pressure three times that of run 6. Despite this, most of the available data tend to indicate that the solid-catalyzed reaction is the principal rate-controlling process. Recent tests to determine the influence of superheater wall material on  $NH_3$  dissociation found that, at a mass rate of 1 mg/sec and 1100°K, the degree of dissociation was 0, 27, 76, and 89% for platinum, Hastelloy, Inconel, and 18:8 stainless, respectively.<sup>8</sup> Dissociation began at approximately 900°K, which is in essential agreement with the present findings as well as data for  $NH_3$  in 304 stainless.<sup>4</sup> The 50% dissociation for run 10 can be attributed to a mass rate which was roughly four times that for run 6. This required a heat flux approximately four times as large as run 6 for the same exit gas temperature, resulting in substantially higher wall temperatures and a correspondingly greater dissociation rate.

Additional effort is required to adequately assess the various mechanisms leading to a rate limitation in the degree of  $NH_3$  dissociation achieved in thrusters of this type. Using well-established chemical engineering techniques, it would be possible to establish design criteria for superheater length, diameter, surface area, and material selection for any set of operating conditions.

### Performance

Although the amount of experimental data obtained was somewhat limited, the general agreement with the correlation

Table 2 Experimental conditions

Run No.	$D^*$ , in.	$\frac{A_e}{A^*}$	$T$ , °F	$F_{ave}$ , $10^{-4}$ lbf	$Re^*$	$I_{sp}$ , lbf-sec/lbm	Propellant
1-3	0.0105	10	275-900	4.3-5.7	400-1200	84-86.3	Amm. carb.
4	0.0324	50	1860	8.0	~120	113	Amm. carb.
6	0.010	100	70-2000	2.8	210-750	68-105	Amm. carb.
7-9	0.010	100	185-195	...	400-10 <sup>4</sup>	...	Nitrogen
10	0.010	100	200-1800	13	600-2400	86-150	Amm. carb.

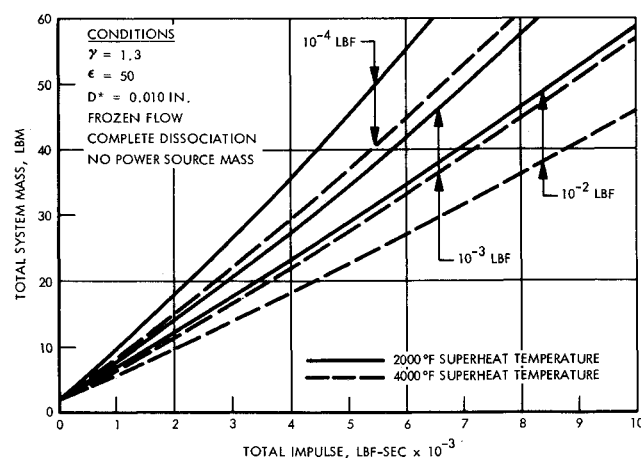


Fig. 5 Total propulsion system mass vs total impulse for ammonium carbamate.

shown in Fig. 3 (bottom) over a fairly wide range of operating conditions indicates that the performance of superheated ammonium carbamate should be predictable to within approximately  $\pm 5\%$ .

A general relationship for throat Reynolds number is given in Ref. 1 as  $Re^* = 4F/\pi\mu D^*\phi_{sp}I_{spt}$ , where  $D^*$  = throat diameter,  $F$  = thrust,  $I_{spt}$  = theoretical specific impulse,  $\mu$  = viscosity, and  $\phi_{sp} = I_{sp}/I_{spt}$ . Using values of  $\phi_{sp}$  from Ref. 1, Fig. 4 was obtained to show the relationship between thrust, throat diameter, nozzle pressure, and delivered specific impulse for temperatures of 2000 and 4000°F. The range of delivered specific impulse values for each  $Re^*$  corresponds to the degree of dissociation obtained. The low number is for no dissociation while the high number is for complete dissociation. It is likely that complete dissociation would be obtained at 4000°F. Figure 4 illustrates the improvement in specific impulse obtained by decreasing the throat diameter for a particular value of thrust. It also shows that a portion of the improvement in the theoretical specific impulse obtained by an increase in temperature is offset by a reduction in  $Re^*$ , and hence  $\phi_{sp}$ , for the same  $D^*$  and  $F$ . The reduction in  $Re^*$  occurs through the decreased mass flow rate and increased viscosity associated with an increase in temperature.

From Fig. 4 it is apparent that specification of the propulsion system mass will be dependent on  $F$ ,  $D^*$ , and temperature for  $Re^* < 10^4$ . Figure 5 illustrates this dependence for ammonium carbamate at the stated conditions. The choice of a 10-mil nozzle was somewhat arbitrary and the performance at the lowest thrust levels could be improved by using a smaller diameter if this were acceptable. The saving in mass with an increase of superheated gas temperature from 2000 to 4000°F is on the order of 30%. An assessment of the power source mass must also be made if this would not normally be available—as has been assumed in Fig. 5.

The total power requirement can be estimated from Fig. 1 by multiplying the theoretical total  $P/F$  by  $F/\phi_{sp}$ . In addition to this, the propellant container and superheater losses must be supplied as well as power for flow control. If a valveless design were used, an additional 1 to 5 w would be required, depending on the operating conditions.<sup>1,9</sup>

### Conclusions

High-performance superheated subliming solid thrusters are feasible by using present resistojet technology to materially increase the specific impulse. Performance comparable to that of  $NH_3$  systems is possible when operated at the same conditions. Where thrust-response times on the order of minutes are acceptable, the 15 to 20% higher  $I_{sp}$  for  $NH_3$  resistojets can be offset by the increased reliability associated with a valveless subliming solid thruster.

### References

- Owens, W. L., Jr., "Design Aspects of Subliming Solid Reaction Control Systems," AIAA Paper 68-516, Atlantic City, N.J., June, 1968.
- White, A. F., "Electrothermal Microthrust Systems," AIAA Paper 67-423, Washington, D.C., 1967.
- Pugmire, T. K., Davis, W. S., and Lund, W., "ATS-III Resistojet Thruster System Performance," *Journal of Spacecraft and Rockets*, Vol. 6, No. 7, July 1969, pp. 790-794.
- Krieve, W. F., "Attitude Control and Stationkeeping Subsystem Program, Final Report," TR AFAPL-TR-68-14, March 1968, TRW Systems Group, Redondo Beach, Calif.
- Page, R. J. and Short, R. A., "Ten-Millipound Resistojet Performance," *Journal of Spacecraft and Rockets*, Vol. 5, No. 7, July 1968, pp. 857-858.
- Cutler, W. H., "Development of a Microthrust Stand for Direct Thrust Measurement," AIAA Paper 68-577, Cleveland, Ohio, June, 1968.
- Kanning, G., "Measured Performance of Water Vapor Jets for Space Vehicle Attitude Control Systems," TN-D-3561, Aug. 1966, NASA.
- Morin, R., private communication, Jan. 1970, Société Européenne de Propulsion, Bordeaux, France.
- Owens, W. L., Jr., "A Flow Control Valve Without Moving Parts," *Proceedings of Fourth Aerospace Mechanisms Symposium*, May 22-23, 1969, Univ. of Santa Clara, Santa Clara, Calif.

## An Experimental and Analytical Study of Film Boiling Heat Transfer to Hydrogen

B. L. PIERCE\* AND J. W. H. CHI†  
Westinghouse Electric Corporation, Pittsburgh, Pa.

EARLY experimental studies on boiling heat transfer to hydrogen involved the measurement of heat fluxes and wall temperatures only. Core et al.<sup>1</sup> and Wright and Walters<sup>2</sup> studied both the nucleate and film boiling regimes but did not correlate their data. Hendricks et al.<sup>3</sup> studied the film boiling regime only and assumed an annular flow model and vapor-liquid equilibrium. They correlated a portion of their data through the use of the Martinelli parameter. In an early attempt to use this correlation to predict fluid and wall temperatures and fluid qualities, we found significant discrepancies between observed and predicted values. Similar results were found by Chenoweth et al.<sup>4</sup>

Presented as Paper 70-660 at the AIAA 6th Propulsion Joint Specialist Conference, San Diego, Calif., June 15-19, 1970; submitted October 16, 1970; revision received February 28, 1971. The Nuclear Engine Rocket Vehicle Application Program (NERVA) is administered by the Space Nuclear Propulsion Office, a joint office of U.S. Atomic Energy Commission and NASA. Aerojet-General Corporation as prime contractor for the engine system and Westinghouse Electric Corporation as subcontractor for the nuclear subsystem, are developing a nuclear propulsion system for space applications. The authors wish to thank E. A. DeZubay who directed the experimental phases of this work, R. W. Graham and J. J. Watt of NASA, J. D. Rogers of LASL, and R. V. Smith of NBS Cryogenic Engineering Laboratory for many helpful discussions during various phases of this program.

\* Fellow Engineer, Systems Engineering, Astronuclear Laboratory.

† Fellow Engineer, Power and Propulsion, Astronuclear Laboratory.